Closed-loop adaptive optics in the human eye

Enrique J. Fernández, Ignacio Iglesias, and Pablo Artal

Laboratorio de Optica, Universidad de Murcia, Campus de Espinardo (Edificio C), 30071 Murcia, Spain

Received January 17, 2000

We have developed a prototype apparatus for real-time closed-loop measurement and correction of aberrations in the human eye. The apparatus uses infrared light to measure the wave-front aberration at 25 Hz with a Hartmann–Shack sensor. Defocus is removed by a motorized optometer, and higher-order aberrations are corrected by a membrane deformable mirror. The device was first tested with an artificial eye. Correction of static aberrations takes approximately five iterations, making the system capable of following aberration changes at 5 Hz. This capability allows one to track most of the aberration dynamics in the eye. Results in living eyes showed effective closed-loop correction of aberrations, with a residual uncorrected wave front of 0.1 μm for a 4.3-mm pupil diameter. Retinal images of a point source in different subjects with and without adaptive correction of aberrations were estimated in real time. The results demonstrate real-time closed-loop correction of aberration in the living eye. An application of this device is as electro-optic "spectacles" to improve vision.

OCIS codes: 330.5370, 010.1080, 330.4460.

The applications of adaptive optics[1] (AO) go beyond astronomy. In particular, AO promises important benefits in visual optics and ophthalmology, for instance, improved vision or increased resolution in ophthalmoscopes. The idea of correcting aberrations in the eye was suggested in the early 1960s by Smirnov,[2] probably independently from previously proposed applications in astronomy. In the late 1980s, the use of a segmented mirror to correct low-order aberrations[3] and the application of techniques similar to speckle interferometry in the eye[4] were antecedents of current research in ophthalmic AO. More recently, static correction of the ocular aberrations by use of deformable mirrors,[5] liquid-crystal spatial light modulators,[6] and phase plates[7] was demonstrated in different laboratories. However, since ocular aberrations change over time,[8] real-time closed-loop correction of aberrations will be required for a variety of practical applications, for instance, in clinical ophthalmology for high-resolution ophthalmoscopes, in scientific applications to carry out new experiments in vision, and in the ophthalmic industry to develop visual simulators. In most of these cases, and unlike for astronomical or military AO applications, a critical factor for ophthalmic AO is the cost of the corrector devices.

In this Letter we report the development of a prototype apparatus for real-time (25-Hz) closed-loop measurement and correction of ocular aberrations that uses as a correction device a relatively low-cost micromachined membrane deformable mirror (MMDM) with 37 channels (control electrodes) from OKO Technologies.[9] This device was proposed for correction of static aberration in an artificial eye[10] and used in closed-loop astronomical applications.[11,12]

Figure 1 shows a schematic diagram of the apparatus. A near-infrared (780-nm) diode laser is used for illumination. A pair of lenses (L_{i1} and L_{i2}, 200- and 50-mm focal lengths) allows focusing of the beam in the retina after reflection in a pellicle beam splitter. In the second pass, after retinal reflection, the light passes another pair of lenses (L_{o1} and L_{o2}, 100- and 200-mm focal lengths) that forms a magnified (2×) image of the pupil on the MMDM. A motorized computer-controlled optometer permits correction of defocus. An additional pair of lenses (L_{o3} and L_{o4}, 200- and 100-mm focal lengths) forms the image of the MMDM (and the eye's pupil without magnification) on the microlenses array of a Hartmann–Shack (HS) sensor[13–15] that measures the ocular aberrations in real time[8] at 25 Hz. We use only a section of MMDM area (8.6 mm in diameter) corresponding to an effective pupil diameter of 4.3 mm in the eye. An additional beam splitter (not included in Fig. 1 for simplicity) is placed after the MMDM, allowing us to record retinal images, or the subject to see a test, after correction of aberrations. The measured ocular aberrations are fitted with 21 Zernike terms, a number suggested to be

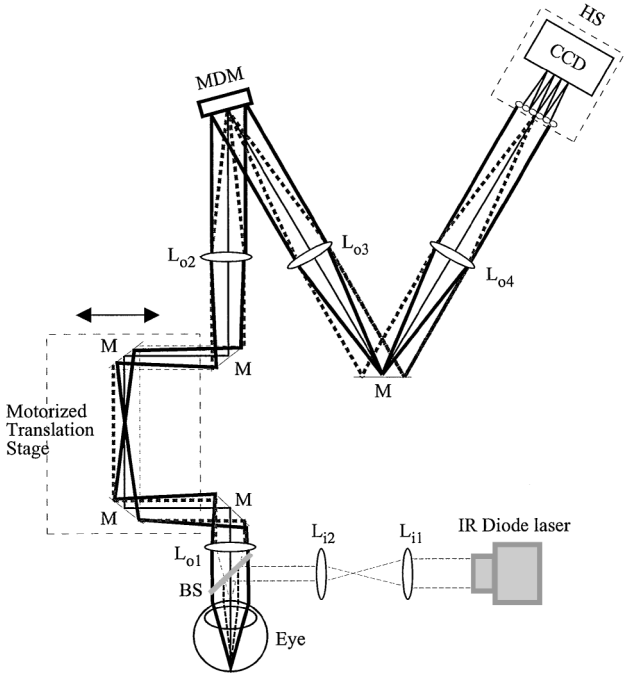

Fig. 1. Schematic diagram (not to scale) of the experimental setup: BS, beam splitter; M, mirrors; MDM, membrane deformable mirror; HS, wave-front sensor.

0146-9592/01/100746-03$15.00/0

adequate for the pupil diameter that was used.[14] In addition, that is the number of modes that can be produced by the MMDM with enough accuracy.

An important factor in this setup is the moderate cost of the components. The HS sensor uses a CCD video camera instead of more-expensive cooled CCD cameras, and, as was mentioned above, the MMDM is less expensive than the deformable mirrors typically used for astronomical applications.

To control the MMDM, we first measured the influence function, $\varphi_l(x, y)$, that represents the membrane shape obtained in response to a voltage applied to a particular electrode (index l). The mirror shape, ΔS, is measured with the HS sensor and can be expressed as a Zernike polynomial expansion:

$$\Delta S = \sum_{k=1}^{M} d_k z_k . \tag{1}$$

However, if we assume that the membrane deformation can be described as a linear superposition of the influence functions, then

$$\Delta S = \sum_{l=1}^{P} c_l \varphi_l . \tag{2}$$

The influence functions are not an orthogonal basis of the membrane deformations. Nevertheless they can also be expressed as a Zernike expansion, where b_{kl} are the elements of a matrix $\mathbf{B}$ that are obtained experimentally by sequential activation of the electrodes and measurement of the mirror shape with the HS sensor. Then, Eq. (2) can be rewritten as

$$\Delta S = \sum_{l=1}^{P} c_l \sum_{k=1}^{M} b_{kl} z_k , \tag{3}$$

and, combining Eqs. (2) and (3), we established a relation between coefficients:

$$d_k = \sum_{l=1}^{P} c_l b_{kl}, \qquad \mathbf{d} = \mathbf{B}\mathbf{c} . \tag{4}$$

Equation (4) states that if one wants to produce a particular mirror shape, e.g., $\mathbf{d}$ vector components, the actuators have to be driven with a set of voltages given by $\mathbf{c}$ components. To compensate the ocular wave front, we applied a recursive approach. Assuming that the HS measurement, $\mathbf{d}_m(t)$, and the change in mirror shape are consecutive within a time interval that is much shorter than the HS measuring rate, the set of voltages is specified by

$$\mathbf{c}(t_n) = M[\mathbf{c}(t_{n-1}) - \mathbf{B}^{-1}\mathbf{d}_m(t_n)] . \tag{5}$$

where M represents a convergence factor and $\mathbf{B}^{-1}$ is the inverse of matrix $\mathbf{B}$, computed with the singular-value decomposition method.[12]

The device was first tested with an artificial eye consisting of a meniscus lens (as the eye's optics) and a rotating diffuser (as an artificial retina). Correction of the static aberrations takes approximately five iterations, rendering the system capable of following changes in aberrations at 5 Hz (with a measurement rate of 25 Hz). This capability permits tracking of most of the aberration dynamics in the eye.[8]

Closed-loop correction of the aberrations was achieved in every normal subject tested so far. Here we present results for two subjects. Figure 2 shows the rms and two Zernike terms (coma and spherical aberrations) as a function of time after activation of closed-loop correction in subject PA. The wave front and the associated PSFs for the first four iterations are also included. The results show effective correction of the aberrations, with a residual uncorrected wave front of ~0.12 μm for a 4.3-mm pupil diameter. This lower value is due mainly to the limitation of the MMDM that produces the desired shape in the convergence algorithm. Figure 3 shows the evolution of the rms with the closed-loop correction activated for a younger subject (EB). In this case, there were some faults in correction, probably because abrupt changes in accommodation were more difficult to

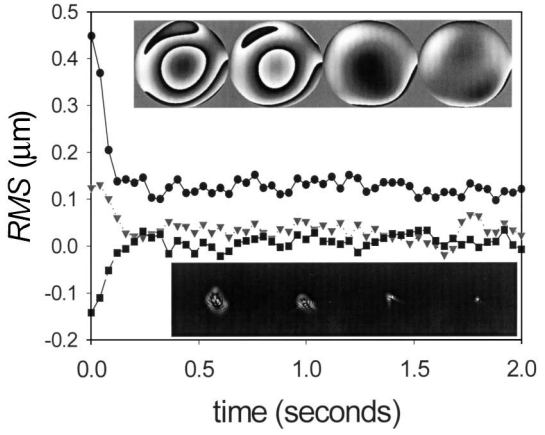

Fig. 2. Evolution of the rms error (circles) and two Zernike coefficients [coma (triangles) and spherical aberrations (squares)] versus time in a human eye (subject PA). A modulus 2π representation of the wave fronts (top inset) and the associated PSFs of the first four iterations in the same experiment (bottom inset) are also included.

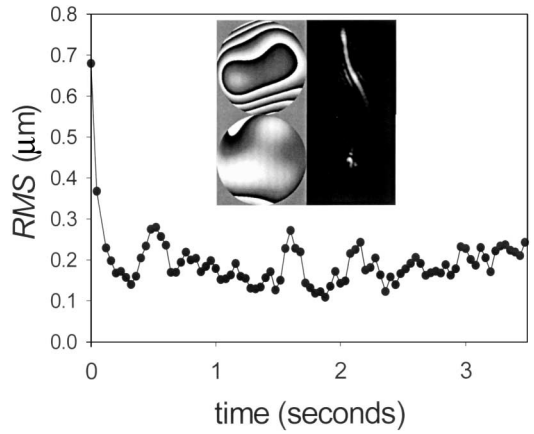

Fig. 3. Evolution of rms error versus time in subject EB. A modulus 2π representation of wave fronts (left-hand inset) and the associated PSFs (right-hand inset) of the first (top) and fourth (bottom) iterations in the same experiment.

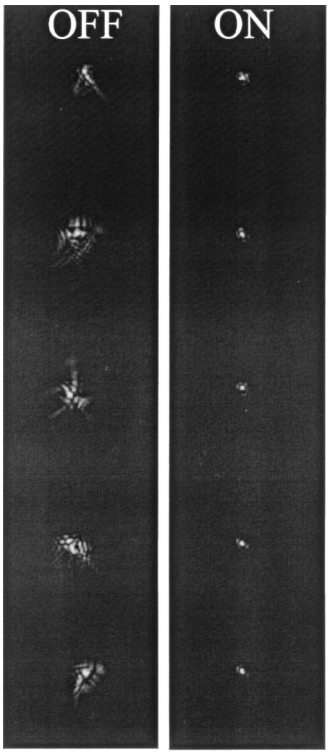

Fig. 4. Series of PSFs taken every 0.2 s, estimated from wave-front data without adaptive correction (OFF) and with closed-loop correction activated (ON). Both series are for subject PA.

follow (the accommodation was not paralyzed). For this subject, the average lower rms was ~0.15 μm but with a larger range of correction (the initial aberration was 0.7 μm). The effect of closed-loop correction can be better appreciated by comparison of a series of real-time retinal images of a point source (computed from the measured wave fronts) with and without adaptive correction of the aberrations. The size and the relative variability of the images provide information on the correction performance. Figure 4 shows a series of retinal images taken every 0.2 s without (OFF) and with (ON) closed-loop correction activated.

A first, and intuitive, application of this device is its use as electro-optic "spectacles" to increase visual acuity in normal subjects. However, this kind of device may also have more important potential benefits in correcting vision in patients with corneal pathologies, for whom conventional optics fail. The system can be also used as a visual simulator to test in advance the effect of aberrations produced by ophthalmic devices or refractive surgery, as well as in high-resolution ophthalmoscopes. In conclusion, a prototype apparatus for real-time closed-loop correction of aberration in the living eye by use of a moderately priced wave-front corrector has been demonstrated.

This research was supported by grant PB97-1056 from the Dirección Generale de Enseñanza Superior Spain. The authors thank Juan L. Aragón and Nicolas Antequera for help with some parts of the software development. P. Artal's e-mail address is pablo@um.es.

References

1. R. K. Tyson, *Principles of Adaptive Optics*, 2nd ed. (Academic, San Diego, Calif., 1997).
2. M. S. Smirnov, Biofizika **6,** 776 (1961).
3. A. W. Dreher, J. F. Bille, and R. N. Weinreb, Appl. Opt. **28,** 804 (1989).
4. P. Artal and R. Navarro, Opt. Lett. **14,** 1098 (1989).
5. J. Liang, D. R. Williams, and D. T. Miller, J. Opt. Soc. Am. A **14,** 2884 (1997).
6. F. Vargas-Martin, P. Prieto, and P. Artal, J. Opt. Soc. Am. A **15,** 2552 (1998).
7. R. Navarro, E. Moreno-Barriuso, S. Bará, and T. Mancebo, Opt. Lett. **25,** 236 (2000).
8. H. J. Hofer, P. Artal, B. Singer, J. L. Aragón, and D. R. Williams, J. Opt. Soc. Am. A **18,** 497 (2001).
9. G. V. Vdovin and P. M. Sarro, Appl. Opt. **34,** 2968 (1995).
10. L. Zhu, P. C. Sun, D. U. Bartsch, W. R. Freeman, and Y. Fainman, Appl. Opt. **38,** 168 (1999).
11. D. S. Dayton, S. Restaino, J. Gonglewski, J. Gallegos, S. MacDermott, S. Browne, S. Rogers, M. Vaidyanathan, and M. Shilko, Opt. Commun. **176,** 339 (2000).
12. C. Paterson, I. Munro, and J. C. Dainty, Opt. Express **6,** 175 (2000), http://epubs.osa.org/opticsexpress.
13. J. Liang, B. Grimm, S. Goelz, and J. F. Bille, J. Opt. Soc. Am. A **11,** 1949 (1994).
14. J. Liang and D. R. Williams, J. Opt. Soc. Am. A **14,** 2873 (1997).
15. P. M. Prieto, F. Vargas-Martín, S. Goelz, and P. Artal, J. Opt. Soc. Am. A **17,** 1388 (2000).